SEDIMENTOLOGY the journal of the International Association of Sedimentologists

Sedimentology (2017) **64**, 1381–1401 doi: 10.1111/sed.12358

Scour holes and ripples occur below the hydraulic smooth to rough transition of movable beds

MAARTEN G. KLEINHANS, JASPER R. F. W. LEUVEN, LISANNE BRAAT and ANNE BAAR
Faculty of Geosciences, Utrecht University, PO-box 80115, 3508 TC, Utrecht, The Netherlands (E-mail: m.g.kleinhans@uu.nl)

Associate Editor – Jaco Baas

ABSTRACT

Scour holes often form in shallow flows over sand on the beach and in morphodynamic scale experiments of river reaches, deltas and estuarine landscapes. The scour holes are on average 2 cm deep and 5 cm long, regardless of the flow depth and appear to occur under similar conditions as current ripples: at low boundary Reynolds numbers, in fine sand and under relatively low sediment mobility. In landscape experiments, where the flow is only about 1 cm deep, such scours may be unrealistically large and have unnatural effects on channel formation, bar pattern and stratigraphy. This study tests the hypotheses that both scours and ripples occur in the same conditions and that the roughness added by sediment saltation explains the difference between the ripple–dune transition and the clear-water hydraulic smooth to rough transition. About 500 experiments are presented with a range of sediment types, sediment mobility and obstructions to provoke scour holes, or removal thereof to assess scour hole persistence. Most experiments confirm that ripples and scour holes both form in the ripple stability field in two different bedform stability diagrams. The experiments also show that scours can be provoked by perturbations even below generalized sediment motion. Moreover, the hydraulic smooth to rough transition modified with saltation roughness depending on sediment mobility was similar in magnitude and in slope to ripple–dune transitions. Given uncertainties in saltation relations, the smooth to rough transitions modified for movable beds are empirically equivalent to the ripple–dune transitions. These results are in agreement with the hypothesis that scours form by turbulence caused by localized flow separation under low boundary Reynolds numbers, and do not form under generalized flow separation over coarser particles and intense sediment saltation. Furthermore, this suggests that ripples are a superposition of two independent forms: periodic bedforms occurring in smooth and rough conditions plus aperiodic scours occurring only in hydraulic smooth conditions.

Keywords Bedform stability, landscape experiments, ripples, scaling, scour holes.

INTRODUCTION: PROBLEM DEFINITION AND OBJECTIVE

Analogue experiments, landscape experiments and scale experiments have frequently been used to investigate fluvial and coastal morphodynamics. Important benefits over field studies are accessibility to materials, processes and sedimentary products for identification and measurement, and the compression of time. These

© 2017 The Authors. *Sedimentology* published by John Wiley & Sons Ltd on behalf of International Association of Sedimentologists

This is an open access article under the terms of the Creative Commons Attribution License, which permits use, distribution and reproduction in any medium, provided the original work is properly cited.

experiments share with numerical models the possibility of control on initial and boundary conditions. On the other hand, by scaling down entire river reaches and deltas to the laboratory, scale problems and distortions arise. Water depth is scaled down by 10^3 to 10^4 times, to mere millimetres or a few centimetre, but it is impossible to scale down particle size by the same factor. These scale issues have been discussed extensively (Reynolds, 1887; Yalin, 1971; Schumm *et al.*, 1987; Peakall *et al.*, 1996; Paola *et al.*, 2009; Kleinhans *et al.*, 2014b).

A potentially problematic issue is the formation of aperiodic scour holes in relatively fine, cohesionless sand; these can, for example, be observed in small-scale 'braided' rivers draining the beach as the tide falls. Ripples form in sufficiently deep flow, but as the discharge reduces the flow becomes shallower and ripples are flattened. However, the scours remain. These scour holes are about 1 to 2 cm deep, 2 to 5 cm wide and 10 cm long, whilst typical flow depths are also about 1 cm (Fig. 1; Kleinhans *et al.*, 2014b). Once initiated, a scour apparently causes flow separation with sufficient turbulence to maintain the scour depth, outcompeting upstream sediment supply to the scour and the direct effect of gravity on sediment mobility on the scour sidewalls, which are near the angle of repose. Here, flow separation includes vortex shedding, which generates turbulence (Venditti *et al.*, 2005b). The scours occur not merely in zones of active transport, such as the migrating channels, but are also provoked by local irregularities and flow confluences in zones where otherwise no or hardly any transport occurs, such as channel margins. However, they are not merely bridge pier scours or confluence scours as found in braided rivers (Ashmore & Parker, 1983) or outer-bend scours in sharp meander bends (Smith, 1998), both of which are forced by external topography or constructions. The shallow-flow scour holes of interest here form internally as a result of local flow and sediment

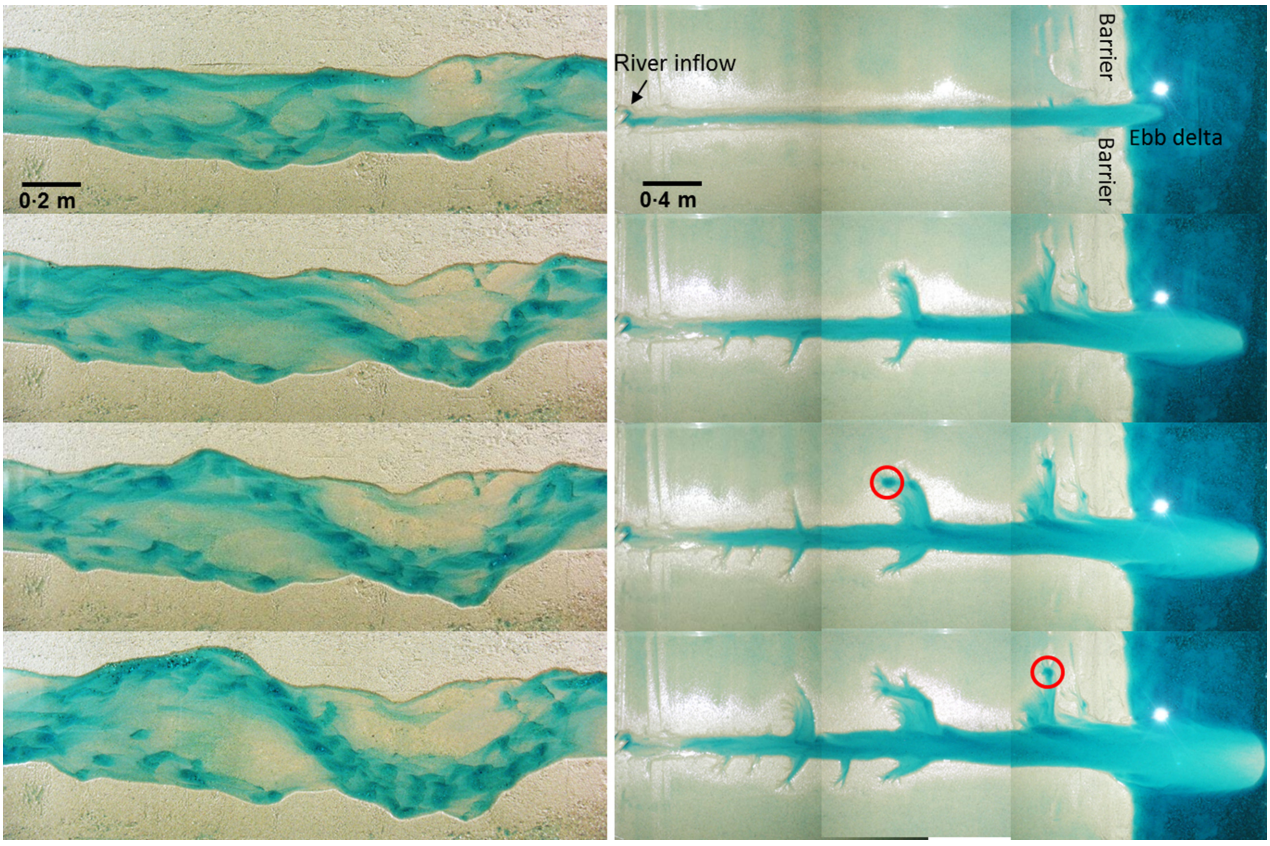

Fig. 1. Tidal experiments with unwanted scour hole formation (left, reach in middle of estuary) or lack thereof (right, entire estuary). White patches are reflections from overhead light. Experiments were conducted as part of student theses (Leuven, 2014; Bartels, 2015). (See Kleinhans *et al.*, 2014a,c, for similar experiments and information on setup.)

© 2017 The Authors. *Sedimentology* published by John Wiley & Sons Ltd on behalf of International Association of Sedimentologists,

interaction; they are quite persistent and, in landscape experiments, unnaturally large. For example, confluences in an experimental tidal network (Stefanon *et al.*, 2010) triggered scour holes of unprecedented depth in nature. These experiments were a breakthrough in tidal systems studies, but to what degree the channel network was affected or even fixated by the scours remains unclear. In the experimental stratigraphic records in Sheets *et al.* (2002) that were used in many subsequent analyses of stratigraphy, interpreted channel deposits were of a similar size as scours. Here, scours may have modified the morphology and stratigraphy but to what degree this affects the generalized conclusions about the set statistics in the stratigraphy is as yet unclear. These scours have no large-scale equivalent; for instance an active meandering river that is 1000 times larger than the experimental river would not have scour holes with flow separation of 20 m deep and 50 m wide in the middle of the typical point bar (van Dijk *et al.*, 2013; Kleinhans *et al.*, 2014b). However, the concern here is that such scours in river and tidal experiments do not merely disfigure local morphology, but modify bar dynamics and stratigraphy and fixate the channel network at the much larger spatial scale. For landscape experiments with such shallow flows that periodic ripples are suppressed and aperiodic scour holes are unwanted, an important question is how to avoid such scours.

Ripples and shallow-flow scours are not always problematic: it can be convenient for scale experiments of channel reaches to have ripples rather than dunes. As dunes tend to have much higher dune height to water depth ratios in laboratory conditions, scaling hydraulic roughness is challenging, whereas ripple dimensions conveniently do not scale with water depth in subcritical flow. In fact, ripples hardly scale with flow conditions (Baas, 1999): once in equilibrium, they have constant dimensions regardless the particle size, flow conditions and geometric scale number of the experiments. In bends, over-large dunes may strongly modify the secondary flow patterns and resulting bar morphology (e.g. Blanckaert *et al.*, 2012), whereas ripples would provide better control whilst allowing higher sediment mobility than in coarser sediment with dunes (Crosato *et al.*, 2012).

Clearly, the tendency to form scours and ripples is important for various types of experiments, and a better understanding of the formation of scours is needed not only to be able to avoid them but also for experiments where ripples are wanted. There is evidence that ripples form as a result of multiple processes, and in relation to scale dependence of the mechanisms there has been debate for decades about the possibly different scaling natures for ripples and dunes (Southard, 1971; Leeder, 1980; Bennett & Best, 1996; Coleman & Nikora, 2011). These processes include the dynamics of the viscous sublayer, interaction between near-bed turbulence and mobile sediment, formation of bed defects or seed waves, and the onset of flow separation. These factors have to some degree been isolated: it is known how moving sediment affects the viscous sublayer in low-mobility (Best *et al.*, 1997) and in the high-mobility sheet flow regimes (Bennett *et al.*, 1998), and it is known how periodic seed waves and bed defects develop (Coleman & Melville, 1996; Venditti *et al.*, 2005b), but there is no current understanding of how scour holes form and self-maintain. Unravelling how multiple processes combine and interact to form ripples is complicated by the fact that the length scale of the seed waves is similar to that of the scours and ripples (Coleman & Melville, 1996; Coleman & Nikora, 2011).

Experiments with flows that are too shallow for ripples but do form scours provide the opportunity to isolate a subset of these processes and additionally gain understanding of the formative conditions of scour holes. The objectives of this study are therefore to experimentally determine under which conditions of flow, particle size and sediment mobility the shallow-flow scours occur, in order to test whether the scours are associated with the hydraulic smooth and transitional regimes and the ripple–dune transition, and whether their occurrence is affected by mobile sediment. Pending a thorough empirical and theoretical basis, this working hypothesis is that the scour phenomenon is related to the hydraulic smooth to rough transition, but is significantly affected by moving sediment.

To this end, the nature of these scours is explored here by using a combination of new data and analysis with literature on turbulence and boundary layer flow, bedform initiation and stability across the ripple–dune threshold, and saltation of bed sediment. In the following sections, the important pieces of the puzzle are combined: observations from the literature of how workers obtained scours or managed to avoid them, measurements of equilibrium

© 2017 The Authors. *Sedimentology* published by John Wiley & Sons Ltd on behalf of International Association of Sedimentologists, *Sedimentology*, **64**, 1381–1401

bedform stability, usually based on many experiments, studies investigating the turbulence characteristics at the ripple–dune transition and effects of sediment transport on near-bed flow, in particular the viscous sublayer. Following review, a predictor is developed from existing theory for the transition from hydraulic smooth to rough conditions affected by particle saltation. The modified hydraulic smooth to rough transition is compared to replotted ripple–dune transitions from two well-supported and frequently used stability diagrams. Then, over 500 small experiments are presented in similar conditions as in analogue and landscape experiments for a wide range of sediments, and with a provocation method to explore the tendency to form and persist scours. Finally, implications for ripples are discussed and effects of poorly sorted sediments on the smooth to rough transition are explored, and recommendations are given on how to obtain or avoid ripples and shallow-flow scours.

HYPOTHESIS AND THEORY DEVELOPMENT

Suggested relations between scours, ripples and the hydraulic smooth to rough transition

The leading hypothesis for the initiation of scour holes is that they form by flow separation and vortex shedding at a local perturbation when the greater part of the mobile bed boundary is hydraulically smooth, which is the case when the particles are embedded in the viscous sublayer (Schlichting, 1968; Best, 1996; Bennett *et al.*, 1998; Coleman & Nikora, 2011). Turbulence forms random perturbations that grow into seed waves of a few particles high (Best, 1996; Coleman & Melville, 1996). The self-generated turbulence by the separated flow in the scour hole then maintains it but the flow apparently reattaches and reforms a boundary layer on the smooth bed. This result contrasts with rough beds where turbulence is generated at the boundary. Note, however, that the hydraulic smooth to rough transition has been defined on the basis of clear-water experiments without moving sediments, and modification of the near-bed flow by moving sediment is significant (Best *et al.*, 1997; Bennett *et al.*, 1998).

Four different practices reported in literature had some success in avoiding scours, and thus indicate a relation of scour formation with moving sediment and bed roughness. Firstly, some experimenters used sand coarser than 0·4 mm and accept the low mobility as representing gravel-bed systems (Tal & Paola, 2010). Secondly, others used fine sediments at relatively high mobility (Davies & Korup, 2007) so that the moving sediment somehow suppressed scouring. As a third alternative, Peakall *et al.* (2007) had hydraulically rough conditions despite the D_{50} being only 0·21 mm. The probable reason for this hydraulic behaviour is that the D_{90} was nearly 2 mm, and Peakall *et al.* (1996) argued that the Reynolds particle number (defined later) should be calculated with the D_{90} rather than the D_{50}. In other words, for poorly sorted sediment the bed is hydraulically rough because of the high roughness length related to the D_{90}, whilst the sediment is conveniently mobile because that is related to the median particle size. Based on this suggestion, Kleinhans *et al.* (2014b) successfully used poorly sorted sand with a significant fraction larger than 0·5 mm. The fourth practice has been to use granular material much coarser than 0·5 mm but with a low density to obtain the required high mobility (Struiksma & Klaassen, 1986; Stefanon *et al.*, 2010; Kleinhans *et al.*, 2014a). Indeed, Tambroni *et al.* (2005) used well-sorted crushed nutshell of 0·3 mm diameter and obtained ripples throughout the experiment. Although these authors suggest that these scale with megaripples observed in natural estuaries, the combination of the low mobility and particle size suggests that they were unwanted current ripples in the hydraulic smooth regime. However, Stefanon *et al.* (2010) used uniform 0·8 mm polystyrene but, surprisingly, obtained morphology dominated by the typical scour holes associated with hydraulically smooth conditions, perhaps because the flow was smooth during most of the tidal cycle.

The above experimental practices to prevent the scour holes suggest that the phenomenon of scouring is related to that of current ripples and disappears with increasing sediment size, increasing skin friction, increasing near-bed flow turbulence and increasing sediment mobility. It has frequently been observed that the hydraulic smooth to rough transition overlaps with the narrow transition from ripples to dunes (Baas, 1994; Bennett & Best, 1996; Venditti *et al.*, 2005b; Schindler & Robert, 2006). Furthermore, a well-known analogous transition is that for settling in still water of fine and coarse sand, where the drag on coarse sand is affected by the

© 2017 The Authors. *Sedimentology* published by John Wiley & Sons Ltd on behalf of International Association of Sedimentologists, *Sedimentology*, **64**, 1381–1401

vortex shedding by the particles (Swamee & Ojha, 1991). Seminal works in the previous century culminated in carefully induced bedform stability diagrams (Southard & Boguchwal, 1990; van den Berg & van Gelder, 1993). Recent studies of the ripple–dune transition, initiation of bed defects and superposition of bedform types indicates that the complex interactions of turbulent flow and well-sorted granular media are far from completely understood (Best, 1996; Bennett *et al.*, 1998; Vendetti *et al.*, 2005; Venditti *et al.*, 2006).

Comparison of ripple–dune transitions in bedform stability diagrams

In the second half of the previous century, workers developed empirical-phase diagrams on the basis of experiments that show the flow regimes and sediment properties in which equilibrium bed states, such as ripples and dunes, are stable (Southard & Boguchwal, 1990; van den Berg & van Gelder, 1993). Such diagrams are useful for two purposes: for assessing the likely bed states in roughly known flow conditions and sediment composition, and to reconstruct the flow conditions from known bed state or sedimentary structures in palaeoterrestrial and extraterrestrial environments. Phase diagrams of bed states thus provide a high-altitude view of bed states and the conditions in which these occur, which is what is needed here, but the diagrams are not intended to replace more detailed models for bedform dimensions and dynamics. The focus here is on the ripple–dune transition and uses the empirically well-supported transitions from some well-known bedform stability diagrams. The transition from ripples to dunes has been debated in the literature, because transitional forms were observed and superposition of ripples on dunes and dunes on dunes (e.g. Ashley, 1990; ten Brinke *et al.*, 1999; Venditti *et al.*, 2005a, 2006; Kleinhans *et al.*, 2007). Consequently, the lines separating the stability fields of ripples and dunes indicate a transition zone rather than a threshold. However, superposition is not important in small-scale landscape experiments.

Seven variables are required to characterize bed states in cohesionless sediment of uniform density and subspherical shape (see Appendix for explanation and well-known equations). Four variables are needed for the flow: water depth, current velocity, and density and viscosity, which slightly depend on temperature and sediment concentration. The sediment is characterized by median grain diameter, the 84th or 90th percentile of the particle size distribution, and density. Because the transition between ripples and dunes, of interest in this paper, is somewhat sensitive to temperature effects, this is taken into account (see Appendix). Further assumptions are approximately logarithmical distributions of sediment sizes, constant hydrodynamic conditions and large water depth (relative to grain size).

Van den Berg & van Gelder (1993) distinguished the same bed states as Southard & Boguchwal (1990). For the purpose of comparison, the lines of the Southard diagram were digitized and plotted in the D_*, θ' space (see Appendix) by assuming the average water depth of the given range and a $k'_s = 2{\cdot}5D_{50}$. Plotted thus (Fig. 2A), the diagrams of Southard for the different water depths are nearly the same for the ripple–dune transition, close at the beginning of motion. There are differences in the dune to upper-stage plane bed (USPB) transition but this is not the focus of the present paper.

The comparability suggests that plotting the Southard diagram with the Shields number related to skin friction adequately collapses the results for different water depths, except for dunes that are known to differ strongly in height relative to water depth between experiments and the field. Moreover, the diagrams of van den Berg and Southard show striking similarities (Fig. 2A), particularly in the position and shape of the transition between the ripple and dune fields and ripples to USPB. To some degree this should come as no surprise because there is overlap in the data sets used for the two diagrams. Furthermore, the triple point of beginning of motion and ripple–dune transition is a 'confusing region of transition' (Southard & Boguchwal, 1973) with very large morphological timescales meaning long experimental waiting times. This region can further be ignored for the present purposes.

Furthermore, a physics-based relation for the beginning of sediment motion was plotted (Vollmer & Kleinhans, 2007; see Appendix; Fig. 2). Here, near-bed turbulence and the dampening effect of the buffer layer causes the well-known dip in the Shields curve near the ripple–dune transition, supporting the idea that the ripple–dune transition is related to the hydraulic smooth to rough transition which also occurs where the buffer layer just about dampens near-bed turbulence production, as plotted on the Shields diagram by Garcia (2000). Next the

© 2017 The Authors. *Sedimentology* published by John Wiley & Sons Ltd on behalf of International Association of Sedimentologists, *Sedimentology*, **64**, 1381–1401

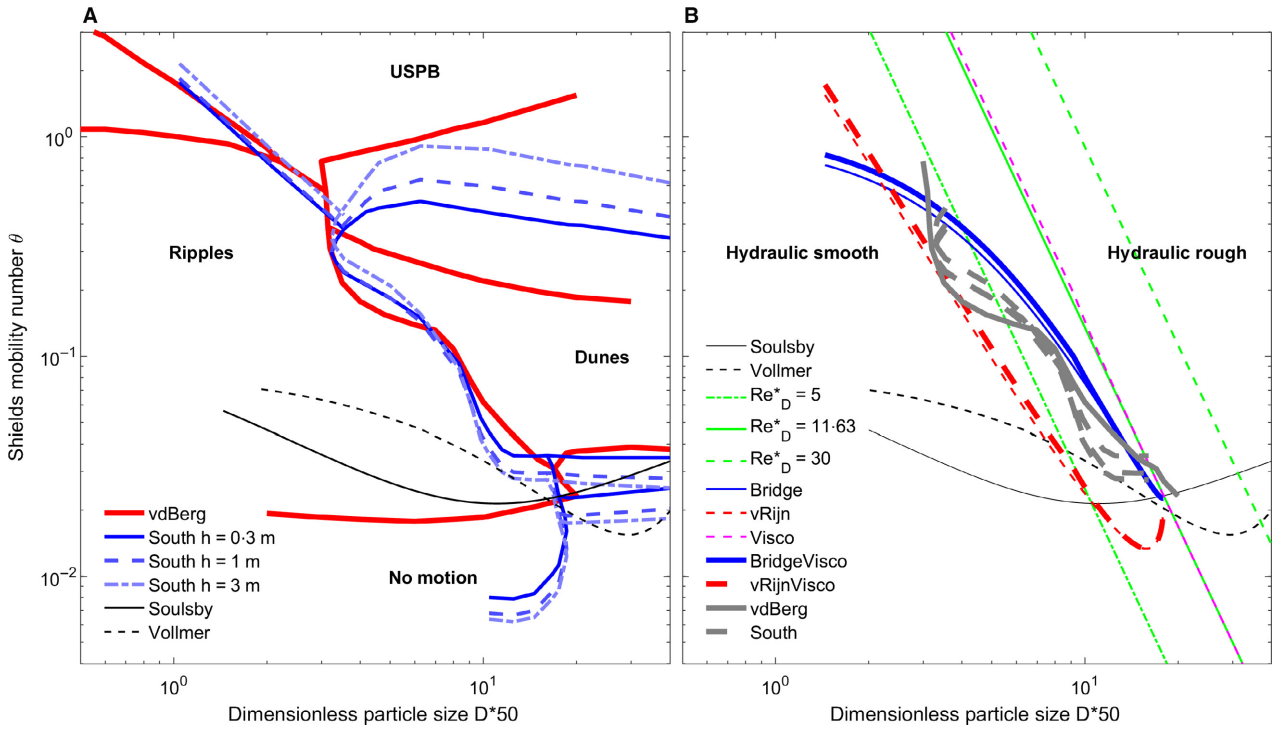

Fig. 2. Empirical bedform stability fields and semi-empirical transitions from hydraulic smooth to rough beds. (A) The similar diagrams of van den Berg & van Gelder (1993) and Southard & Boguchwal (1990) for three water depths are shown with the four main stability fields 'no motion', upper-stage plane bed (USPB), ripples and dunes indicated. The Soulsby (1997) 'Shields curve' for generalized sediment motion is close to the lower lines of the empirical stability diagrams. (B) Transitions from hydraulic smooth to rough boundaries compared to the empirical ripple–dune transitions. The three lines for different $Re*_D$ bracket the empirical smooth to rough transitions for clear-water flow. For the line $Re*_D = 11{\cdot}63$, the limited effect of added viscosity by bedload concentration is shown. Effects of added roughness by the saltation layer are shown in bold for the van Rijn (1984a) and Bridge & Bennett (1992) models, combined with the added viscosity effect, which is insignificant.

smooth to rough transition will be compared to the ripple–dune transition and the effect of added bed roughness due to particle saltation will be assessed.

Hydraulic smooth to rough transition

The current image of the viscous sublayer is based on time-averaged measurements above smooth walls, where a linear velocity profile has been observed that grades into the logarithmic, Kármán-Prandtl law of the wall, the log-layer, where the transition is often called the buffer layer (Schlichting, 1968; Bennett *et al.*, 1998). The process underlying the change in behaviour from smooth to rough beds is flow separation. Because this process is still the subject of active research, the present study will proceed from a simplified image on the basis of the above review and Best (1996), as follows. At a rough wall with particles emerging from the viscous sublayer, minute vortices are shed from all roughness elements, whereas at a smooth wall with particles well submerged in the viscous sublayer such turbulence generation does not occur except at perturbations. Also along the crests of ripples, downstream of the reattachment zone of the separated flow, the bed is thought to be smooth or transitional but not rough.

This image suggests that in order to obtain a fully rough sediment bed, there need to be sufficient close-spaced perturbations. This understanding has long been applied by artificially roughening air foils, golf balls and so on to suppress flow separation. Specifically, localized roughness elements higher than the viscous sublayer cause localized flow separation. Flow separation, in turn, is then suggested to lead to self-maintaining scour holes and ripples with large separation cells. Such roughness elements include seed waves and other perturbations (Southard & Dingler, 1971; Coleman & Melville, 1996; Venditti *et al.*, 2005b). In mobile sediment in laminar flow, bedforms initiate from self-

© 2017 The Authors. *Sedimentology* published by John Wiley & Sons Ltd on behalf of International Association of Sedimentologists,

formed defects or wavelets that, when large enough, start to cause flow separation (Venditti *et al.*, 2005b). Once flow separation sets in, the enhanced turbulence may cause more sediment transport, trough and scour formation and bedform growth. However, also below the threshold for motion, scour can be initiated: Southard & Dingler (1971) empirically found an inverse relation between shear stress and the required mound height for ripple initiation, suggesting that in fine sand flow separation is localized at bedform crests of sufficient amplitude, where self-maintaining scours may then form in conjunction with the wavelets to form ripples. On the other hand, coarse sand and poorly sorted medium sand foregoes the existence of a viscous sublayer by causing ubiquitous flow separation at a small scale, which acts effectively as a separation inhibitor in a similar manner to the rough surface on air foils and golf balls (Leeder, 1980). Generally, ubiquitous roughness elements, such as wavelets and large particles, cause generalized small-scale flow separation with enhanced overall turbulence, which suppresses large separation cells with self-maintaining scour holes and ripples.

The transition from a hydraulically smooth bed to a rough bed occurs where the viscous sublayer is suppressed. The thickness of the sublayer has been derived in the past from a transition in the clear-water velocity profile over a smooth boundary: the flow in the viscous sublayer is about laminar with a linear velocity profile, whereas that in the turbulent boundary layer above it has a logarithmic distribution (see Schlichting, 1968, for theory). The transition takes place over some distance, but the fitted linear and logarithmic velocity profiles intersect at boundary Reynolds number $\mathrm{Re}_* = 11{\cdot}63$, where:

$$\mathrm{Re}_* = \frac{u_* k_\mathrm{s}}{\nu} \tag{1}$$

in which $u_* = \sqrt{\tau/\rho}$, shear velocity and k_s is the height of the roughness elements, such as particles, wavelets, scour holes or other perturbations. On average, the viscous sublayer thickness (m) in clear water is given as

$$\delta \approx \frac{\nu \mathrm{Re}_*}{u_*} \tag{2}$$

For typical conditions and sediments at the beginning of motion $\delta \approx 0{\cdot}8$ mm for $\mathrm{Re}_* = 11{\cdot}63$ and $\theta_\mathrm{c} = 0{\cdot}02$, and $\delta \approx 0{\cdot}5$ mm for $\theta_\mathrm{c} = 0{\cdot}04$. However, in reality the layer thickness fluctuates due to turbulence in the flow over it. A buffer layer is observed between $5 < \mathrm{Re}_* < 30$ and, more conservatively, $3{\cdot}5 < \mathrm{Re}_* < 70$. This layer covers the range where the flow is neither linearly nor logarithmically varying with elevation above the boundary, and empirical relations are used for this range (Nezu & Azuma, 2014). This range also coincides with the 'low' in the Shields curve (Zanke, 2003; Vollmer & Kleinhans, 2007). So, for flow separation with vortex shedding and near-bed resulting turbulence to occur requires bed roughness lengths to be larger than δ. The question is then what the appropriate boundary Reynolds number is.

The transition from smooth to rough can be plotted in the Shields–Bonnefille number space (see Appendix) assuming a value for the boundary Reynolds number $\mathrm{Re}_{*\mathrm{sr}}$ and D_{50} as roughness length. Eqs 1 and 18 are now combined as:

$$\theta_\mathrm{sr} = \left(\frac{\nu \mathrm{Re}_{*\mathrm{sr}}}{k_\mathrm{s}}\right)^2 \frac{\rho}{(\rho_\mathrm{s} - \rho) g D_{50}} \tag{3}$$

The three lines for $\mathrm{Re}_{*\mathrm{sr}} = [5, 11{\cdot}63, 30]$ bracket a wider transition from smooth to rough than where the transition from ripples to dunes is empirically found to be (Fig. 2B). A line at $\mathrm{Re}_{*\mathrm{sr}} \approx 5$ is closest to the empirical transitions in the bedform stability diagrams (Kleinhans, 2005a,b). This agrees with other observations that the onset of flow separation occurs at $\mathrm{Re}_{*\mathrm{sr}} > 4{\cdot}5$ (Williams & Kemp 1971, in Best, 1996; Venditti *et al.*, 2005b). This result may mean that for flow over sediments the $\mathrm{Re}_{*\mathrm{sr}} = 11{\cdot}63$ criterion is overly strict or that the actual bed roughness is higher than the D_{50}. However, not only the magnitude is incorrect, but additionally the smooth to rough transition is steeper than the ripple–dune transitions. Furthermore, there is a kink in the ripple–dune transitions at intermediate mobility that does not occur in the smooth to rough transition. The transition will now be modified for movable beds.

Modified hydraulic smooth to rough transition for saltating sediment

The aforementioned differences between ripple–dune transitions and the clear-water smooth to rough transition could have a number of causes that cannot easily be captured in a simple

© 2017 The Authors. *Sedimentology* published by John Wiley & Sons Ltd on behalf of International Association of Sedimentologists, *Sedimentology*, **64**, 1381–1401

function, including the complex changes in the turbulence field at the transition from ripples to dunes, and the modification of the boundary layer properties by the moving sediment (Best *et al.*, 1997; Bennett *et al.*, 1998; Nezu & Azuma, 2014). Since the interest here is a type of experiment where dunes will not occur due to the low water depth, only the effects of saltating bedload sediment on the roughness k_s and on the viscosity v are explored to predict the effect of saltation on the transition from smooth to rough flow.

Detailed measurements of sediment-laden flow show that flow velocity and turbulence intensity in the buffer layer are increasingly enhanced by coarser moving sediment relative to clear-water flow (Best *et al.*, 1997; Bennett *et al.*, 1998; Nezu & Azuma, 2014). This tendency increases towards the bed at distances smaller than $15u_*/v$, suggesting an upper value for the transition range of $\mathrm{Re}_{*sr} = 15$ rather than 30 or even 70 for the definition of the buffer layer. Effectively this flattens the velocity profile, which can also simplistically be interpreted as a necessity to shift the theoretical profile upward by the added roughness. Nezu & Azuma (2014) interprets the change of velocity profile as a modification of the Kármán constant as a function of sediment concentration, but Bennett *et al.* (1998) argued that modifications of the viscosity or roughness length are empirically equally valid.

Viscosity increases when sediment is added (e.g. Bennett *et al.*, 1998) which can be accounted for by constitutive relations for kinematic viscosity v_c and flow density ρ_c depending on sediment concentration in the saltating bedload layer:

$$\rho_c = \rho + C(\rho_s - \rho) \tag{4}$$

and:

$$\mu_c = \mu\left(1 + 2{\cdot}5C + 6{\cdot}25C^2 + 15{\cdot}62C^3\right) \tag{5}$$

where C [−] is the volumetric bedload concentration estimated by the van Rijn (1984b) relation for reference concentration:

$$C = 0{\cdot}015\frac{D_{50}}{k_s}\left(\frac{\theta' - \theta_c}{\theta_c}\right)^{1{\cdot}5} D_*^{-0{\cdot}3} \tag{6}$$

Effective dynamic viscosity $v_c = \mu_c/\rho_c$ increases with concentration, so the effect is a decrease of the actual Re_{*sr}. A cumbersome plotting method would then be to correct all data and shift it to the left in the bedform stability diagrams with $\theta' - D_*$ space. Instead, the data are straightforwardly plotted, but the function is corrected before plotting by multiplying the right-hand side of Eq. 1 with a factor v_c/v, as shown in Fig. 2. The effect of sediment concentration on the Reynolds boundary number is surprisingly small for the $\mathrm{Re}_* = 11{\cdot}63$ line, and the line becomes a little steeper than the ripple–dune transitions, which is the opposite of the required correction. A correction of the Kármán constant κ, to be multiplied with the shear velocity, as a function of concentration would have had a similar small effect because κ reduces only 5% for the relevant concentration range (Nezu & Azuma, 2014).

The second effect of saltating bedload on the viscous sublayer thickness considered here is adding roughness by the saltation layer. Following Bridge & Bennett (1992), roughness length k_s is assumed to equal the saltation height plus the particle size, which can be estimated as:

$$\frac{k_s}{D} = 2{\cdot}53(\theta' - \theta_c)^{0{\cdot}5} + 1 \tag{7}$$

where $k_s \approx D$ at the threshold for motion. As an alternative, the saltation height function of van Rijn (1984a) was applied:

$$\frac{k_s}{D} = 0{\cdot}3\left(\frac{\theta' - \theta_c}{\theta_c}\right)^{0{\cdot}5} D_*^{0{\cdot}7} + 1 \tag{8}$$

An independent piece of evidence supporting the idea that saltation height adds roughness is found in the case of gravity wave boundary layers in the coastal zone. Here, the movement of particles on a flat bed has been found to increase the effective roughness as a function of the square root of mobility number, the same power as in current-related bedload (eq. 3.6.10 in Nielsen, 1992):

$$\frac{k_s}{D} = 170\sqrt{\theta' - \theta_c} \tag{9}$$

However, the importance of saltation for the problem herein is unique to subaqueous flows: in wind the entire problem of this paper is irrelevant because here saltation jump length is known to cause small wind ripples, whereas saltation height is independent of the shear velocity and orders of magnitude larger than the

© 2017 The Authors. *Sedimentology* published by John Wiley & Sons Ltd on behalf of International Association of Sedimentologists, *Sedimentology*, **64**, 1381–1401

laminar sublayer (Rasmussen *et al.*, 2015), suggesting that in flows more viscous than water the saltation roughness may differ, which is perhaps relevant for future interpretations of landscape experiments with laminar flow. Whether this means that scour holes such as those studied here cannot occur in air or other planetary atmospheres is beyond the scope of this paper.

Saltation height in water increases with Shields number, so the effect is an increase of the actual Re_{*sr}; this is plotted in the bedform stability diagrams with $\theta' - D_*$ space using Eq. 3, and for input, and by multiplication of 1/2·5 to correct for the fact that Eq. 3 assumes $k_s = D_{50}$ whereas the saltation relations should use $k_s = 2{\cdot}5D_{50}$ or a higher percentile of the particle size distribution. The smooth to rough transition is corrected for plotting by multiplying the right-hand side of Eq. 1 with D/k_s. The effect of saltation on the modification of the smooth to rough transition is large, as shown in Fig. 2 for the $Re_* = 11{\cdot}63$ line. As a result, the transitions calculated with the Bridge and the van Rijn relations bracket the empirical lines from the bedform stability diagrams. The considerable difference between the two different saltation models reflects the uncertainty of bedload sediment transport prediction. Given this uncertainty, these findings are not at odds with the observations by Nezu & Azuma (2014) that the depth below which sediment–flow interactions are most significant commences at $Re_* = 15$, whilst frequently cited upper limits for hydraulically rough flow of $Re_* = 30$ or even $Re_* = 70$ are overly conservative.

From the above, it must be concluded that the hydraulic smooth to rough transition modified with saltation is empirically the same as the ripple–dune transitions in the bedform stability diagrams, which is more due to the uncertainty in saltation height than due to the uncertainty in the ripple–dune transition. Despite the uncertainty, the modified transition is considerably better matched to the ripple–dune transition than the clear-water smooth to rough transition. The remainder of the paper therefore labours under the assumption that the ripple–dune transition and the modified smooth to rough transition, including roughness by saltating particles, have the same cause. To test whether scour holes do not occur above these transitions, new experiments are presented in conditions similar to those in landscape experiments in the next section.

SCOUR EXPERIMENTS IN A RANGE OF SEDIMENTS

Methods and materials

The experiments were done in a similar way to those in Southard & Dingler (1971) and Venditti *et al.* (2005b), starting in every case from a plane bed of homogenized sediment. The bed was screed as smooth as possible and perturbed to possibly initiate scour and ripple formation. With the large spatial variation in shear stress in landscape experiments in mind, conditions need to be included well below the beginning of sediment motion; this requires a hard perturbation to cause flow separation and turbulence, rather than a soft one as in Venditti *et al.* (2005b). To this end, scour was provoked by a cylindrical, emergent object placed vertically in the sediment and studied whether, after removal, the scour caused by it was self-maintained.

The experiments were done in a straight flume 0·4 m wide with controllable discharge that was measured. In all sets of experiments, a sediment bed about 2 m long and 5 cm thick was installed. The beds were exposed to a range of flow discharges with depths of a few centimetres (measured by ruler) to bracket sediment mobility from well below to well above motion. Critical and supercritical flow conditions were excluded from the analysis. The Shields sediment mobility number varied between 0·007 and 0·67. Water temperature ranged between 11°C and 15°C.

Experiments were conducted with a range of readily available sediment mixtures (Table 1; Fig. 3) used in experiments published elsewhere, from well-sorted fine beach sand to poorly sorted river sands with median diameters ranging between 0·19 mm and 0·46 mm and D_{90} up to 1·40 mm. All sediments were cohesionless. To test the effects of sorting, variations on the poorly sorted river sediment ('river1') were made: the coarsest sediment was sieved out ('river2'), and a sediment ('river0') was newly mixed where also the finest sediment is absent. The 'river0' sediment is more angular and from a different source.

Furthermore, typical low-density sediments with median diameters ranging between 0·57 mm and 2·05 mm and with densities from 1055 to 1300 kg m^{-3} were included that are used in landscape experiments; this included crushed walnut shell that has been used in the past for scale models, and polystyrene particles used at

© 2017 The Authors. *Sedimentology* published by John Wiley & Sons Ltd on behalf of International Association of Sedimentologists, *Sedimentology*, **64**, 1381–1401

Table 1. Sediments used in the more than 500 experiments. See Fig. 3 for particle size distributions. References indicate in which of the present experiments these sediments were used before.

Name	n	D_*	D_{50} (mm)	D_{90} (mm)	ρ_s (kg m^{-3})	Depth (cm)	Discharge (m^3 h^{-1})	Source experiments
River0	30	11·1	0·46	1·15	2650	4·0	1·6–42·5	na
River1	86	10·9	0·42	1·40	2650	3·1–12·0	3·5–40·1	van Dijk *et al.* (2012)
River2	40	10·0	0·46	1·11	2650	2·8–7·8	6·4–42·1	van Dijk *et al.* (2013)
Fine skew	27	6·5	0·27	0·69	2650	2·5–6·3	5·6–34·1	na
Beach	36	4·9	0·19	0·29	2650	0·6–1·1	0·9–23·3	van Dijk *et al.* (2012)
Nutshell	21	20·3	1·49	1·70	1300	4·0	2·6–21·5	na
Polystyrene	42	15·6	2·05	2·66	1055	5·0	3·0–10·0	Kleinhans *et al.* (2014a)
Light1	20	18·3	1·40	1·70	1200	4·2	0·7–18·0	na
Light1·5	36	12·6	1·02	1·29	1200	5·0	3·0–14·8	na
Light2	54	11·7	0·71	0·92	1200	4·0–9·5	5·4–36·0	na
Light3	48	7·1	0·58	0·68	1200	4·9	2·9–13·5	na
Lightmix1	43	6·5	0·57	1·15	1200	4–10·5	5·3–30·0	Marra *et al.* (2014)
Lightmix2	55	12·6	1·09	1·36	1200	5·0	3·1–15·0	na

the BundesAnstalt für Gewässerkunde, both well-sorted. Well-sorted polymer sediments were used here, as well as a poorly sorted sediment successfully used in Marra *et al.* (2014) that was composed from the well-sorted sediments. Furthermore, experiments were conducted with a poorly sorted sediment ('lightmix2') with a similar size distribution as the 'river2' sand.

Visual observations and interventions were made in the middle of the bed, as far as possible from the boundaries. The tendency to form scours was firstly studied by observing whether sediment was mobile and scours formed in shallow flow or whether incipient ripples formed in somewhat deeper flow. The response to interventions was studied: scours usually formed when an emergent cylindrical obstacle was placed in the bed, even when the sediment bed was just about static, and after removal it was observed whether the scour disappeared or continued to exist. Equilibrium of the ripple fields was not pursued, which would have taken much more time, because in the authors' experience

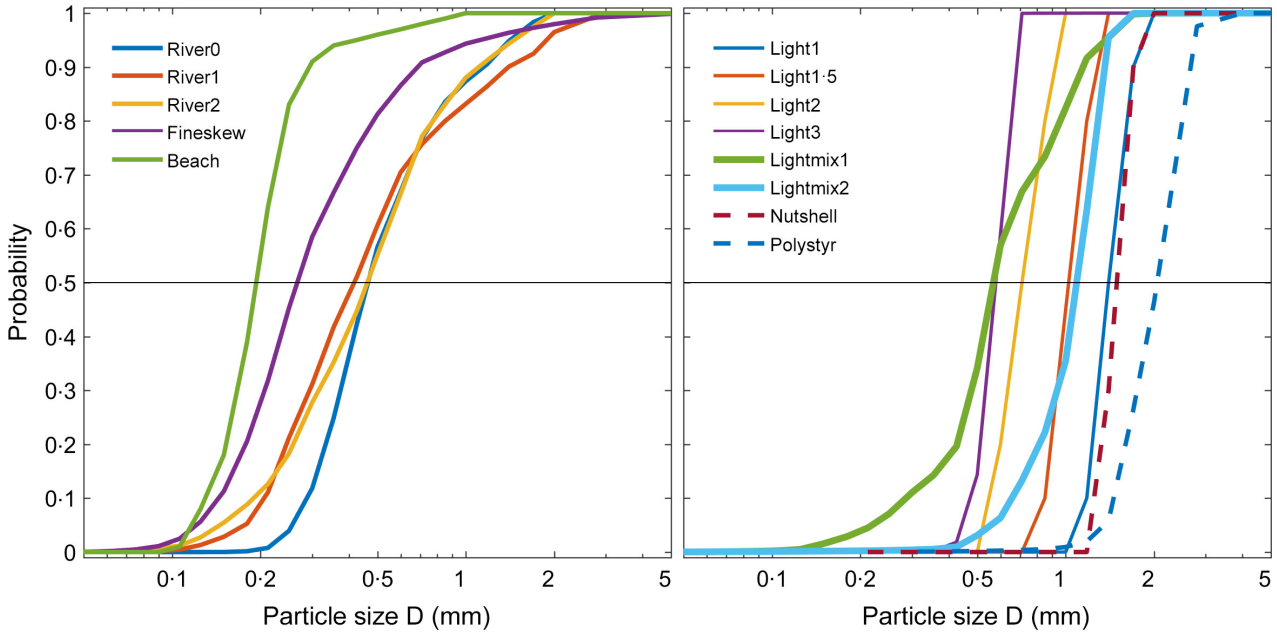

Fig. 3. Cumulative particle size distributions of the used sediments. See Table 1 for other sediment properties.

© 2017 The Authors. *Sedimentology* published by John Wiley & Sons Ltd on behalf of International Association of Sedimentologists, *Sedimentology*, **64**, 1381–1401

and in the paraphrased words of Bagnold 'ripples spread like a disease' and persist once they initiate. The bed was photographed in some experiments for all sediments. Five classes of behaviour were observed and noted: no (generalized) sediment motion ('nomotion' in the figure legends), sediment motion over a planar bed ('noscours'), which can be low and high intensity, self-forming ripples or scours without provocation ('ripples'), and for provoked scours whether they continued to exist ('provstay') or filled in ('provfill').

Care was taken to continue the observations in low-mobility conditions long enough for morphological change to occur. Experiments were terminated when bedforms triggered by the upstream sand bed ramp arrived at the test section. Consequently, some experiments that might have developed self-maintained scours and ripples when given enough time now plot as no ripples, which may also cause some of the scatter. The distinction between the classes 'provstay' and 'provfill' was difficult and subjective for the lowest mobilities, but as the focus is on the transition in somewhat higher mobilities this does not affect the main conclusions of the paper. Finally, given that experiments for different sediments were done by different authors and that visibility of the scours varied with sediment type, there is bound to be some subjectivity in this classification, which possibly causes some scatter or outliers.

Results

All sediments near the beginning of motion formed scours when provoked with an obstacle (Fig. 4). Provoked scours had shapes typical for scour around cylinders with rapid deepening upstream of the obstacle and more gradual shallowing downstream of the obstacle. The scoured sediment formed a deposit further downstream that sometimes had a spur and often had a downstream-facing slipface. Measured dimensions of the scours are as expected from observations in landscape experiments (Fig. 5), with depths of about 1 to 2 cm, widths of 2 to 8 cm and lengths of 5 to 10 cm and no discernable relation with sediment type or mobility. Obstacle diameter had a minor effect: scour holes provoked by larger obstacles were a bit more pronounced (Fig. 6).

The majority of the observed bed states, here including the scours, plot in the correct stability field (Fig. 7). The correct plotting of the 'no motion' conditions supports that the experiments and data reduction were done correctly. The scatter at the smooth to rough transition is about a factor two. A few provoked scours also plot in the no motion field due to sediment entrainment by the local turbulence caused by the obstacle and observed as sediment transport events. Ripples and scours scatter somewhat over the smooth–rough boundary. In some experiments, removal of the obstacle led to filling of the scour over time, without forming other scours (Fig. 8), whilst in other experiments the scours continued to exist and sometimes caused ripple formation. Of the provoked scours, nearly all that continued to exist after obstacle removal plot below the modified smooth–rough criteria including saltation effects on roughness (Fig. 9).

Some observations plot in the wrong stability field for reasons explained below. Some self-formed scours plot above the smooth–rough criteria. In all cases except for the river0 sediment discussed below, the mismatch occurs for the

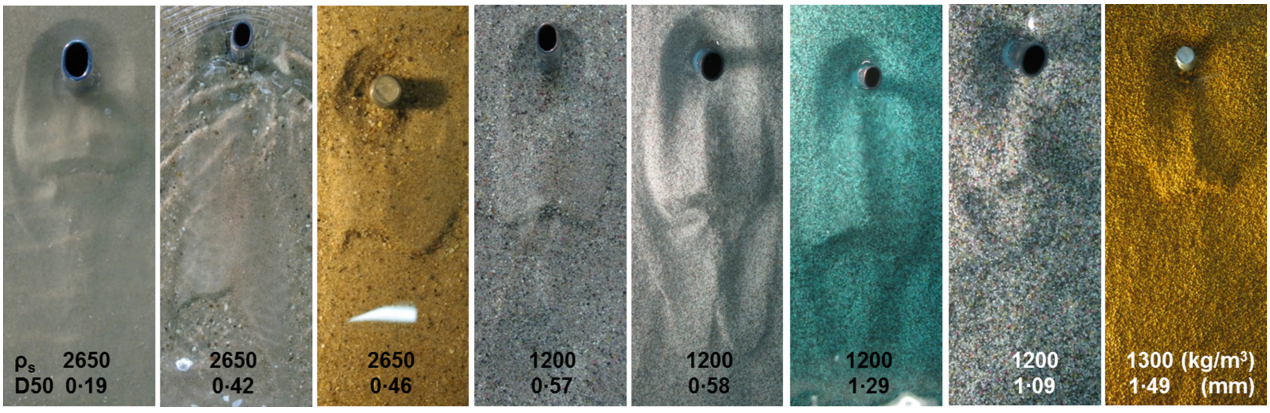

Fig. 4. Similar scour holes in a range of sediments provoked by an obstacle. Sediment density and median particle size are indicated. White patches are reflections from overhead light.

© 2017 The Authors. *Sedimentology* published by John Wiley & Sons Ltd on behalf of International Association of Sedimentologists, *Sedimentology*, **64**, 1381–1401

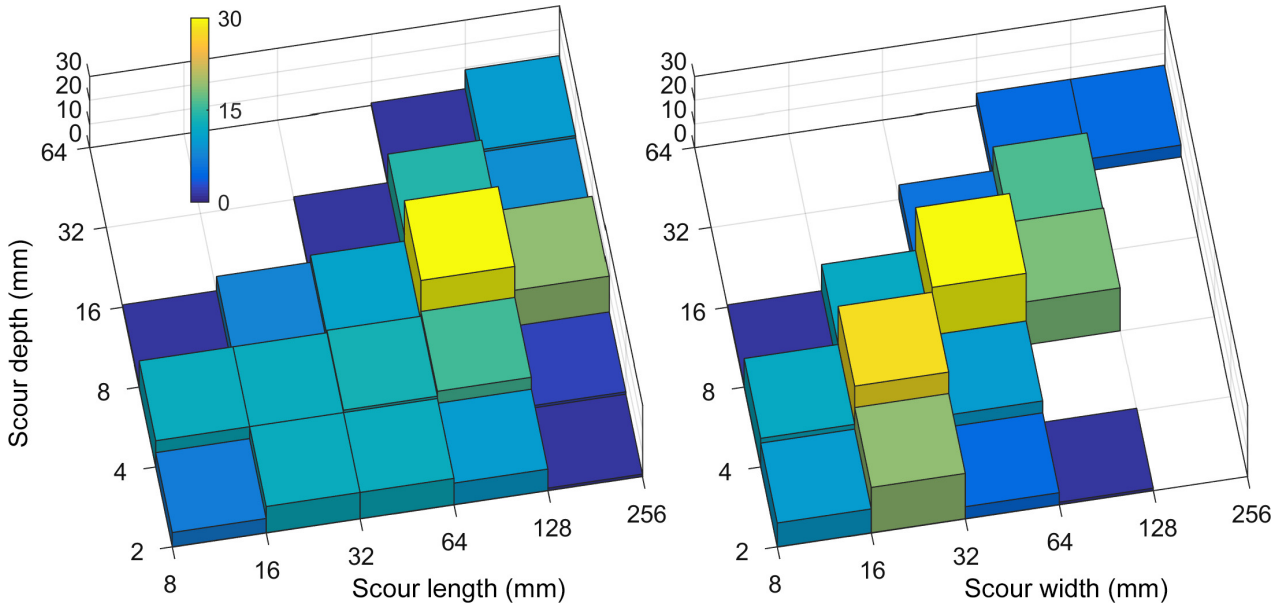

Fig. 5. Histogram of measured scour hole depth, length and width in all experiments. No trends were found with sediment properties and flow conditions.

same type of low-density sediment. This result is in agreement with observations in Marra *et al.* (2014) of a tendency to form surprisingly deep scours in run-off channels, particularly in the bends where flow separation caused additional turbulence. The cause of this unexpected behaviour in this type of sediment remains unclear. Nevertheless, most provoked scours disappear in the low-density mixture 'lightmix2' that was designed to mimic the size distribution of the 'river2' sand, suggesting that poorer sorting reduces the tendency to form scours.

The distinction between incipient ripples with trough scours on the one hand and wavelets without trough scours on the other hand was not always clear and somewhat subjective; this may explain why several 'ripple' observations occur in the dune field, for example for the walnut sediment. The scours provoked in the walnut sediment disappear above the smooth to rough transition; yet the same condition without provoked scours caused ripples; this seeming contradiction leads to the suggestion that these 'ripples' may have been misinterpreted seed waves, but this remains uncertain.

Another exception is that some ripples formed in the river0 sediment. Size segregation was observed where ripples formed in the fine sediment patches, and indeed in pilot landscape experiments not reported here the bed became covered in ripples and scours where fine sediment had segregated. In contrast, in the river1 and river2 sediments the provoked scours disappear as expected above the smooth to rough transition, but the provoked scours in the river0 sediment did not disappear. This sediment has the same size distribution as the river2 sediment, except that its finer tail is coarser and it is a more angular sand from a different source, meaning that the tendency to scour of the river0 sediment was expected to be less, rather than more than in the river2 sediment; this points to the need to have unimodal, symmetrically logarithmically distributed sediments such that there is equal mobility of all size fractions (*sensu* Parker & Klingeman, 1982).

In summary, assuming that the explanations here for the anomalous points are correct, the modified smooth to rough transitions and the ripple–dune transitions separate the majority of experiments with and without persistent scours. For the purposes of design of landscape experiments, a simple relation for unimodal, rather well-sorted sediments is plotted (Fig. 7) above which scours generally do not occur:

$$\theta \approx 6D_{*50}^{-2} \tag{10}$$

This is the minimum mobility condition needed for analogue and landscape experiments without unwanted scours, or the maximum mobility condition when scours are wanted. This relation differs from the relation proposed by Peakall

© 2017 The Authors. *Sedimentology* published by John Wiley & Sons Ltd on behalf of International Association of Sedimentologists, *Sedimentology*, **64**, 1381–1401

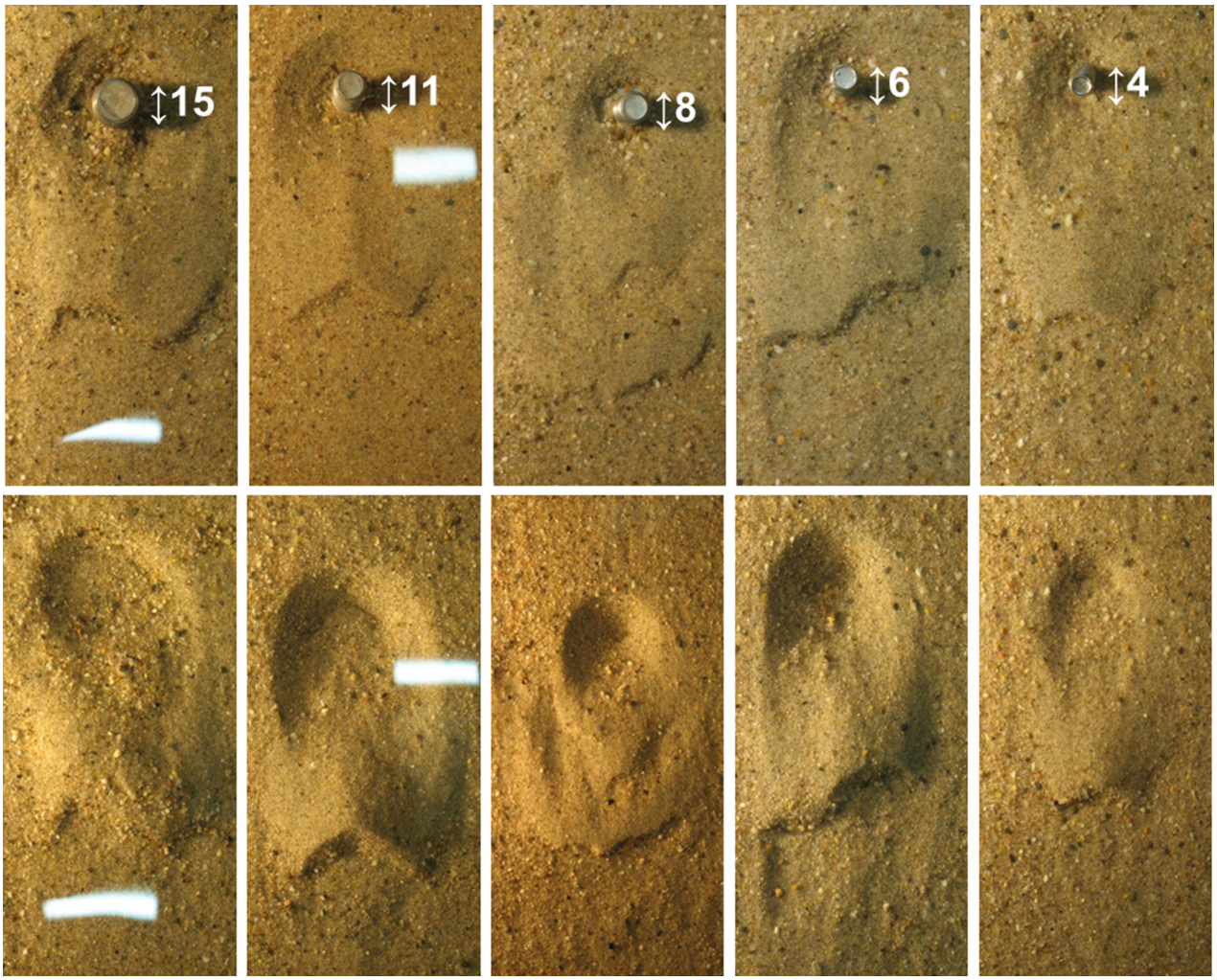

Fig. 6. Similar scour holes for a range of obstacle diameters (indicated). The experiment was done in poorly sorted sand with D_{50} = 0·43 mm at a velocity of 0·269 m s^{-1} below the threshold for motion. White patches are reflections from overhead light.

et al. (1996) that was based on the clear-water smooth to rough transition. For the most common laboratory conditions with sand of the usual density of 2650 kg m^{-3} and a water temperature of 15°C, this relation can be simplified to:

$$\theta \approx 0{\cdot}011 D_{50}^{-2}, \qquad (11)$$

with D_{50} in millimetres.

DISCUSSION

Conditions conducive to scour hole formation

The self-forming ripples and scours generally plot below the modified hydraulic smooth to rough criterion, which is close to the transition from ripples to dunes unlike the clear-water smooth to rough transition. This effect is interpreted to mean that the scours were self-maintained and indeed flow separation and much stronger turbulence in such scours were observed than around it. On the other hand, above the smooth–rough criterion nearly all provoked scours filled and disappeared after obstacle removal, meaning that these were not self-maintained. These findings are positive evidence for the modification of the transition from hydraulically smooth to rough conditions by saltation roughness, which deviates not merely in magnitude but in slope from the clear-water criterion.

Also the provoked scours that self-maintained after obstacle removal plot correctly in this field, while the provoked scours that disappear after removal of the obstacle plot in the rough/dune

© 2017 The Authors. *Sedimentology* published by John Wiley & Sons Ltd on behalf of International Association of Sedimentologists, *Sedimentology*, **64**, 1381–1401

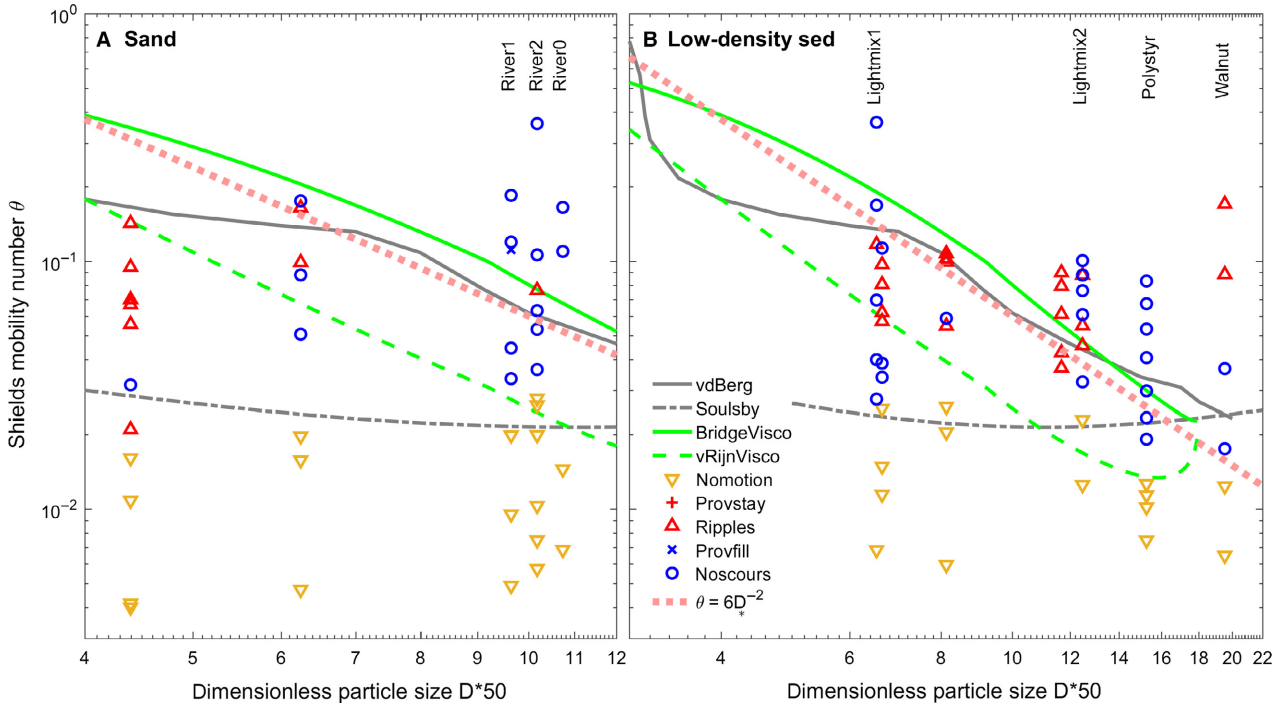

Fig. 7. Experimental data of bed states with transitions of hydraulic smooth to rough bed indicated. (A) Only sand. (B) Low-density sediments. Vertically aligned data indicate sets with one sediment. Poorly sorted sediments are indicated. See text for the simple empirical rule above which scours are unlikely to occur.

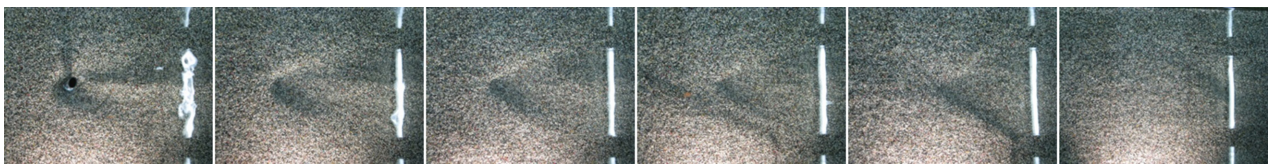

Fig. 8. Refilling scour hole after removal of the 15 mm obstacle. The experiment was done with low-density sediment of 1200 kg m^{-3} with D_{50} = 1·6 mm at a velocity of 0·167 m s^{-1}. White patches are reflections from overhead light.

field where localized flow separation is expected to be suppressed. However, in one low-density sediment persistent scours or ripples occurred above the suggested threshold and in some coarse sands ripples were observed, although these may have been wavelets or local ripples in fine sand patches, which points to the transitional nature of the smooth to rough transition discussed above.

The results of this study have possible implications for the long-debated ripple–dune transition. These findings show that the stability fields of scours and ripples are empirically the same and the transition is the same as the modified hydraulic smooth to rough transition, except in that there is a kink in the bedform stability lines at higher mobility that is not explained by the added roughness by saltation. The ripple–dune transition clearly occurs as a result of multiple processes, where added roughness by saltation is empirically sufficient to explain the difference between the clear-water smooth to rough transition and the ripple–dune transition for lower mobilities. Given that seed waves emerge in hydraulic smooth and rough conditions, and can therefore potentially develop into larger periodic bedforms (Best, 1996; Coleman & Nikora, 2011), the present authors suggest that it is the emergence of aperiodic scours that makes the difference between ripples and dunes: perhaps ripples are a superposition of self-maintaining, aperiodic scours and periodic bedforms, where the scours are so dominantly present that they suppress possible relations between bedform dimensions and flow characteristics. Perhaps the rather constant scour

© 2017 The Authors. *Sedimentology* published by John Wiley & Sons Ltd on behalf of International Association of Sedimentologists, *Sedimentology*, **64**, 1381–1401

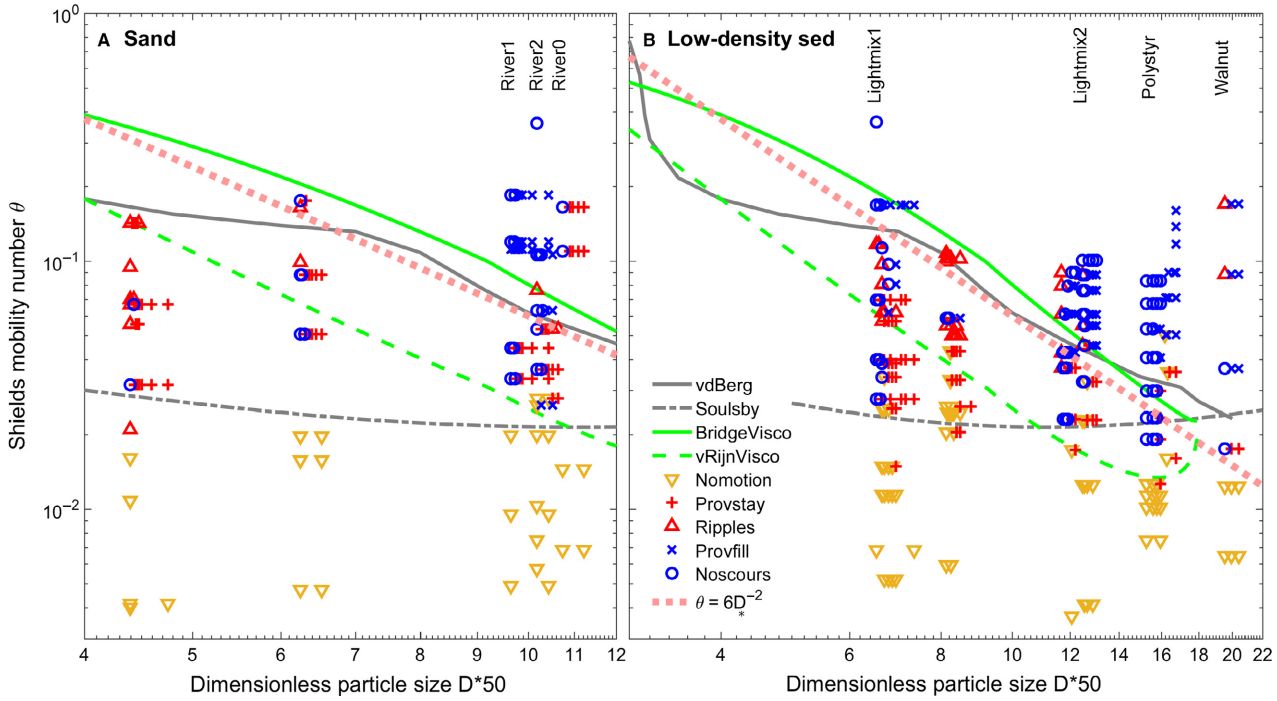

Fig. 9. Same as Fig. 7, but now including all provoked experiments. (A) Only sand. (B) Low-density sediments. Vertically aligned data indicate sets with one sediment. Horizontally aligned data show experiments with increasing obstacle size, which are incrementally shifted to the right for visibility.

dimensions control the wavelength of ripples, whereas shallow-flow scours in the absence of ripples may have any spacing, but this needs further dedicated experimentation. From this line of thought, it follows that dunes are fundamentally the same bedforms as the ripples, but without the scours, and dunes can therefore attain dimensions in relation to the flow conditions where this tendency is inevitably overwhelmed by the scours in the case of ripples. These results lead to new questions about scale experiments in engineering context. If the flow and roughness and bedform dimensions are so different in dune and ripple-related conditions, then perhaps their effects on the scaling of scour depth in bends and around bridge piers and groynes need better understanding.

Use of poorly sorted sediment to create optimal roughness

Literature and present experiments suggest that a wide sediment mixture is conducive to the suppression of scour holes and ripples in agreement with Peakall *et al.* (1996) and Kleinhans *et al.* (2014b), but this appears to be quite sensitive to the precise composition. The river0 sand (Table 1) was composed so that it resembled the river1 sediment but with less coarse sediment and without any silt or clay and, indeed, the slightly finer sand had ripples above the expected threshold where the river1 sediment did not, which is shown in Fig. 7A around $D_* = 11$. Mobility is also quite important: near the threshold for motion, the river1 sediment that was successfully used for river experiments without scours (van Dijk *et al.*, 2012, 2013) was prone to provoked scour formation. Both of these points illustrate the sensitivity of the scouring process to minor changes in sediment composition, particularly the coarse tail of the distribution, and sediment mobility.

Here, the suggestion by Peakall *et al.* (1996) that the 90th percentile by weight should then be used in the Reynolds boundary number is explored further. The question is whether this agrees with the idea of optimal surface roughness for full coverage of the bed with turbulent flow (Cebeci & Smith, 1974), which suppresses localized flow separation at scour holes; this is taken to be the condition wherein the flow is hydraulically rough.

The size and spacing of roughness elements determines the added turbulence: a general rule is that the length of the separated flow zone is about five times the height of the element

© 2017 The Authors. *Sedimentology* published by John Wiley & Sons Ltd on behalf of International Association of Sedimentologists, *Sedimentology*, **64**, 1381–1401

causing the flow separation. Interpreting this as the maximum spacing by roughness elements to cover the entire bed in wake turbulence, the minimum coverage fraction is about 0·2. This result agrees well with data by Cebeci & Smith (1974) of measured roughness over transverse ribs, where an optimum spatial coverage fraction of 0·1 to 0·25 caused the highest roughness. However, roughness elements closer together interact to reduce drag and Brayshaw *et al.* (1983) measured an optimal spacing of three roughness element heights, meaning a coverage fraction of 0·33; this, in turn, can be interpreted as that in order to be rough a sediment bed needs a surface fraction of 0·1 to 0·33 covered by roughness elements that cause flow turbulence with vortex shedding because they protrude above the viscous sublayer.

This study calculated which size fraction in the particle size distribution by volume corresponds to the optimal surface fraction of roughness elements for ubiquitous flow separation. Unimodal, lognormally distributed sediments are defined with D_{50} = 0·5 mm and a range of standard deviations. Firstly, the theoretical cumulative distributions were converted from volume (and mass, assuming the same density of all fractions) to surface area occupied. Next, a correction was applied on the distribution for dynamic armouring at the surface, which causes the larger particles to be relatively more abundant (Marion & Fraccarollo, 1998; also see Kleinhans, 2005a). Clearly, the larger particles are less abundant at the surface by coverage area (solid lines in Fig. 10A) than by mass (dashed lines in Fig. 10A). Finally, the percentile of the larger particles occupying the optimal area was calculated, here by fractions 0·1, 0·2 and 0·33. The result is that the percentile of optimal area for rough flow decreases as the mixture becomes more poorly sorted (solid lines in Fig. 10B). In other words, optimal bed roughness is not well represented by the D_{90} as first suggested by Peakall *et al.* (1996) but by a percentile that depends on the mixture standard deviation.

This result needs further modification because the size of the roughness elements should not be below D > 0·5 mm for which the bed is thought to be just about rough. The percentile by volume (and mass) was calculated for which D = 0·5 mm

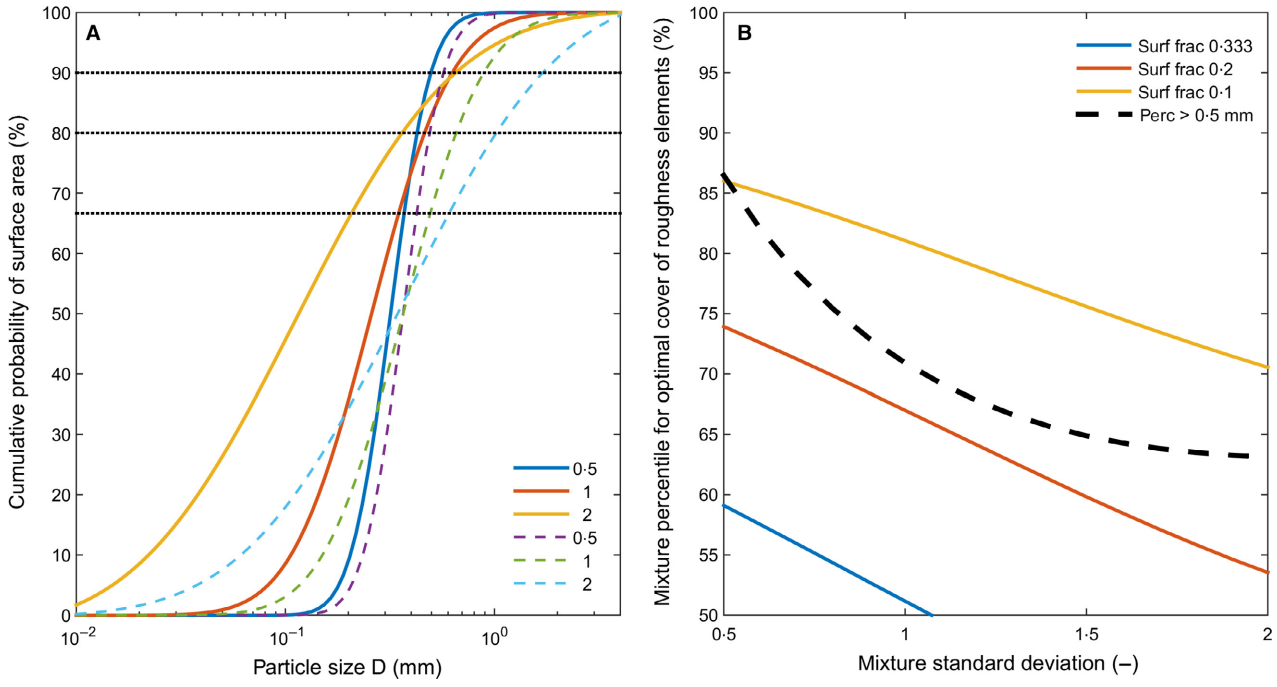

Fig. 10. Surface area covered by larger particles as roughness elements for sediment mixtures with a median size of 0·5 mm. (A) Probability density of surface area covered by particles for a range of mixture standard deviations. Dashed lines indicate the probability density by volume (and mass) for the best and poorest sorted mixture. The range for optimal spatial coverage for the highest roughness is indicated. (B) Sediment mixture percentiles by volume (and mass) for optimal roughness as a function of mixture standard deviation, showing that particles of lower percentiles contribute to the roughness for poorer sorting.

© 2017 The Authors. *Sedimentology* published by John Wiley & Sons Ltd on behalf of International Association of Sedimentologists,

(dashed line in Fig. 10B), showing that in all the larger particles occupying 25% of the surface (blue line) are not large enough to cause flow separation because they plot below the $D = 0{\cdot}5$ mm line, while those occupying only 10% (red line) are more than large enough for all standard deviations except the smallest. These results show that the 90th percentile is an overestimation of what is needed for ubiquitous flow separation over moderately to poorly sorted sands with $D_{50} = 0{\cdot}5$ mm. More precisely, percentiles lower than D_{90} apply for wider mixtures as long as they protrude above the viscous sublayer. However, this result is contrary to the observations: it suggests that in wider mixtures a percentile closer to the median should be used, which reduces rather than increases the boundary Reynolds number. Moreover, the slope of the line with constant $\mathrm{Re}_{*\mathrm{sr}}$ is clearly different from that of the ripple–dune transitions, which leads to the conclusion that assuming a high percentile diameter in the calculation of the smooth to rough transition for sediment mixtures is underestimating the roughness more, the poorer the sorting of the mixture. Nevertheless, the analysis and the experiments show that somewhat poorly sorted sediments can be used to advantage in landscape experiments to reduce the tendency to form scours if the sediment is unimodal as to promote equal mobility of all size fractions.

CONCLUSIONS

A large data set was collected from experiments with self-formed scours about 2 cm deep, covering a large range of conditions, particle sizes and densities. Scour holes have dimensions independent of flow conditions and particle properties. Scours were also provoked by obstacles that were subsequently removed to investigate whether the scours are self-maintaining.

Self-formed and provoked scours disappear with increasing particle size and sediment mobility above a threshold related to the transition of hydraulic smooth to rough boundaries. However, this is not the classical clear-water relation with $\mathrm{Re}_* \approx 11{\cdot}63$ and effective roughness based on median particle size. Rather, the smooth to rough transition occurs at lower Shields numbers and smaller particles than expected for clear-water conditions because sediment saltation causes additional roughness. Here, saltation height and roughness depend on Shields number. This result agrees well with earlier work showing that saltation modifies the buffer layer and effectively adds roughness. On the other hand, added viscosity due to bedload sediment concentration has a negligible effect.

The effective roughness in the smooth to rough transition depends also on the surface proportion of particles larger than the viscous sublayer thickness, which depends on the mixture standard deviation; this explains suggestions in the literature that the smooth to rough transition is best estimated with some large percentile of the particle size distribution, but a single percentile is not empirically adequate.

For the purpose of design of landscape experiments wherein scours are required or unwanted, a simple empirical function above which scours should not occur was induced for sand: $\theta \approx 0{\cdot}011 D_{50}^{-2}$ with D_{50} in millimetres.

The results support hypotheses that saltation and self-maintaining scour holes with flow separation are important for the ripple–dune transition: bedforms in fine sediment have superimposed scours, which together form three-dimensional current ripples with dimensions nearly independent of flow conditions, whereas bedforms in coarse sediment do not form scours and can attain dimensions related to flow conditions. The findings of this study were generalized to the testable hypothesize that ripples are a superposition of periodic bedforms and aperiodic scours.

ACKNOWLEDGEMENTS

We acknowledge critical reviews by Sean Bennett and Arjan Reesink and steer by Associate Editor Jaco Baas. Wouter Marra, Wim Uijttewaal, Mohamed Nabi, Eveline van der Deijl, Sean Bennett and Keld Rasmussen are thanked for discussion in early stages of this work. MGK was supported by the Netherlands Organisation for Scientific Research (NWO) (grants ALW-Vidi-864.08.007 to MGK). The other authors were funded by student fellowships of the Netherlands Royal Academy of Arts and Sciences to the Board of Education of the Earth Science graduate school. This work was encouraged by the Sediment Experimentalist Network.

REFERENCES

Ashley, G.M. (1990) Classification of large-scale subaqueous bedforms: a new look at an old problem. *J. Sediment. Petrol.*, **60**, 160–172.

© 2017 The Authors. *Sedimentology* published by John Wiley & Sons Ltd on behalf of International Association of Sedimentologists, *Sedimentology*, **64**, 1381–1401

Ashmore, P. and **Parker, G.** (1983) Confluence scour in coarse braided streams. *Water Resour. Res.*, **19**, 392–402.

Baas, J.H. (1994) A flume study of the development and equilibrium morphology of current ripples in very fine sand. *Sedimentology*, **41**, 185–209.

Baas, J.H. (1999) An empirical model for the development and equilibrium morphology of current ripples in fine sand. *Sedimentology*, **46**, 123–138.

Bartels, P. (2015) Ups-and-downs of tidal systems: formation and development of ebb- and flood tidal channels and bars. Master thesis, Faculty of Geosciences, Universiteit Utrecht, The Netherlands. Available at: http://dspace.library.uu.nl/handle/1874/323470.

Bennett, S. and **Best, J.** (1996) *Mean Flow and Turbulence Structure Over Fixed Ripples and the Ripple-Dune Transition*, pp. 281–304. Wiley, Chichester.

Bennett, S., **Bridge, J.** and **Best, J.** (1998) Fluid and sediment dynamics of upper stage plane beds. *J. Geophys. Res.*, **103** (C1), 1239–1274.

van den Berg, J. and **van Gelder, A.** (1993) A new bedform stability diagram, with emphasis on the transition of ripples to plane bed in flows over fine sand and silt. Publs Int. Ass. Sediment. Vol. 17. International Association of Sedimentologists, pp. 11–21.

van den Berg, J. and **Van Gelder, A.** (1998) Discussion: Flow and sediment transport over large subaqueous dunes: Fraser River, Canada. *Sedimentology*, **45**, 217–221.

Best, J. (1996) *The Fluid Dynamics of Small-Scale Alluvial Bedforms*, No. 3. Wiley, Chichester, pp. 67–126.

Best, J., **Bennett, S.**, **Bridge, J.** and **Leeder, M.** (1997) Turbulence modulation and particle velocities over flat sand beds at low transport rates. *J. Hydraul. Eng.*, **123**, 1118–1129.

Blanckaert, K., **Kleinhans, M.G.**, **McLelland, S.J.**, **Uijttewaal, W.S.J.**, **Murphy, B.J.**, **van der Kruijs, A.**, **Parsons, D.R.** and **Chen, Q.** (2012) Flow separation at the inner (convex) and outer (concave) banks of constant-width and widening open-channel bends. *Earth Surf. Proc. Landforms* **38**, 696–716.

Brayshaw, A., **Frostick, L.** and **Reid, I.** (1983) The hydrodynamics of particle clusters and sediment entrainment in coarse alluvial channels. *Sedimentology*, **30**, 137–143.

Bridge, J. and **Bennett, S.** (1992) A model for the entrainment and transport of sediment grains of mixed sizes, shapes and densities. *Water Resour. Res.*, **28**, 337–363.

ten Brinke, W., **Wilbers, A.** and **Wesseling, C.** (1999) Dune growth, decay and migration rates during a large-magnitude flood at a sand and mixed sand-gravel bed in the dutch rhine river system. *Spec. Publ. Int. Assem. Sediment.*, **28**, 15–32.

Cebeci, T. and **Smith, A.** (1974) *Analysis of Turbulent Boundary Layers*. Academic Press, New York, NY, USA.

Coleman, S. and **Melville, B.** (1996) Initiation of bed forms on a flat sand bed. *J. Hydraul. Eng.*, **122**, 301–310.

Coleman, S. and **Nikora, V.** (2011) Fluvial dunes: initiation, characterization, flow structure. *Earth Surf. Proc. Landforms*, **36**, 39–57.

Crosato, A., **Desta, F.**, **Cornelisse, J.**, **Schuurman, F.** and **Uijttewaal, W.** (2012) Experimental and numerical findings on the long-term evolution of migrating alternate bars in alluvial channels. *Water Resour. Res.*, **48**, W06524.

Davies, T. and **Korup, O.** (2007) Persistent alluvial fanhead trenching resulting from large, infrequent sediment inputs. *Earth Surf. Proc. Landforms*, **32**, 725–742.

van Dijk, W.M., **Van de Lageweg, W.I.** and **Kleinhans, M.G.** (2012) Experimental meandering river with chute cutoffs. *J. Geophys. Res.*, **117**, F03023.

van Dijk, W.M., **Van de Lageweg, W.I.** and **Kleinhans, M.G.** (2013) Formation of a cohesive floodplain in a dynamic experimental meandering river. *Earth Surf. Proc. Land.*, **38**, 1550–1565.

Garcia, M. (2000) The legend of a.f. shields, discussion by marcelo h. garcia. *J. Hydraul. Eng.*, **126**, 718–720.

Kleinhans, M.G. (2005a) Flow discharge and sediment transport models for estimating a minimum timescale of hydrological activity and channel and delta formation on Mars. *J. Geophys. Res.*, **110**, E12003.

Kleinhans, M.G. (2005b) Phase diagrams of bed states in steady, unsteady, oscillatory and mixed flows. In: *Sandpit Project* (Eds L.C. Van Rijn, R.L. Soulsby, P. Hoekstra and A. Davies), pp. Q1–Q16. Aqua Publications, Amsterdam, The Netherlands.

Kleinhans, M.G. and **Van Rijn, L.C.** (2002) Stochastic prediction of sediment transport in sand-gravel bed rivers. *J. Hydraul. Eng.*, **128**, 412–425.

Kleinhans, M.G., **Wilbers, A.** and **ten Brinke, W.** (2007) Opposite hysteresis of sand and gravel transport up- and downstream of a bifurcation during a flood in the River Rhine, The Netherlands. *Netherl. J. Geosci.*, **86**, 273–285.

Kleinhans, M.G., **Terwisscha van Scheltinga, R.**, **van der Vegt, M.** and **Markies, H.** (2014a) Turning the tide: growth and dynamics of a tidal basin and inlet in experiments. *J. Geophys. Res. Earth Surf.*, **120**, 95–119.

Kleinhans, M.G., **van Dijk, W.**, **van de Lageweg, W.**, **Hoyal, D.**, **Markies, H.**, **van Maarseveen, M.**, **Roosendaal, C.**, **van Weesep, W.**, **van Breemen, D.**, **Hoendervoogt, R.** and **Cheshier, N.** (2014b) Quantifiable effectiveness of experimental scaling of river- and delta morphodynamics and stratigraphy. *Earth Sci. Rev.*, **133**, 43–61.

Kleinhans, M.G., **van Rosmalen, T.**, **Roosendaal, C.** and **van der Vegt, M.** (2014c) Turning the tide: mutually evasive ebb- and flood-dominant channels and bars in an experimental estuary. *Adv. Geosci.*, **39**, 21–26.

Leeder, M. (1980) On the stability of lower stage plane beds and the absence of current ripples in coarse sands. *J. Geol. Soc. London*, **137**, 423–429.

Leuven, J.R.F.W. (2014) Turning the tide: The effect of river discharge on estuary dynamics and equilibrium. Master thesis, Faculty of Geosciences, Universiteit Utrecht, The Netherlands. Available at: http://dspace.library.uu.nl/handle/1874/301306.

Marion, A. and **Fraccarollo, L.** (1998) A new conversion model for areal sampling of fluvial sediments. *J. Hydraul. Eng.*, **123**, 1148–1151.

Marra, W., **Braat, L.**, **Baar, A.** and **Kleinhans, M.G.** (2014) Valley formation by groundwater seepage, pressurized groundwater outbursts and crater-lake overflow in flume experiments with implications for Mars. *Icarus*, **232**, 97–117.

Nezu, I. and **Azuma, R.** (2014) Turbulence characteristics and interaction between particles and fluid in particle-laden open channel flows. *J. Hydraul. Eng.*, **130**, 988–1001.

Nielsen, P. (1992) *Coastal Bottom Boundary Layers and Sediment Transport*. No. 4 in Advanced Series on Ocean Engineering. World Scientific, Singapore.

Paola, C., **Straub, K.**, **Mohrig, D.** and **Reinhardt, L.** (2009) The "unreasonable effectiveness" of stratigraphic and geomorphic experiments. *Earth Sci. Rev.*, **97**, 1–43.

© 2017 The Authors. *Sedimentology* published by John Wiley & Sons Ltd on behalf of International Association of Sedimentologists, *Sedimentology*, **64**, 1381–1401

Parker, G. and **Klingeman, P.** (1982) On why gravel bed streams are paved. *Water Resour. Res.*, **18**, 1409–1423.
Peakall, J., **Ashworth, P.** and **Best, J.** (1996) Physical modelling in fluvial geomorphology: principles, applications and unresolved issues. In: *The Scientific Nature of Geomorphology* (Eds B. Rhoads and C. Thorn), pp. 221–253. Wiley, Chichester, UK.
Peakall, J., **Ashworth, P.** and **Best, J.** (2007) Meander-bend evolution, alluvial architecture, and the role of cohesion in sinuous river channels: a flume study. *J. Sediment. Res.*, **77**, 197–212.
Rasmussen, K., **Valance, A.** and **Merrison, J.** (2015) Laboratory studies of aeolian sediment transport processes on planetary surfaces. *Geomorphology*, **244**, 74–94.
Reynolds, O. (1887) On certain laws relating to the regime of rivers and estuaries and on the possibility of experiments on a small scale. *Br. Assoc. Rep. London*, 555–562.
van Rijn, L. (1984a) Sediment transport, part I: bed load transport. *J. Hydraul. Eng.*, **110**, 1431–1456.
van Rijn, L. (1984b) Sediment transport, part II: suspended load transport. *J. Hydraul. Eng.*, **110**, 1613–1641.
Schindler, R. and **Robert, A.** (2006) Flow and turbulence structure across the ripple-dune transition: an experiment under mobile bed conditions. *Sedimentology*, **52**, 627–649.
Schlichting, H. (1968) *Boundary-Layer Theory*, 6th edn. McGraw-Hill, New York, NY, USA.
Schumm, S., **Mosley, M.** and **Weaver, W.** (1987) *Experimental Fluvial Geomorphology*. Wiley, New York, NY, USA, 413 pp.
Sheets, B.A., **Hickson, T.A.** and **Paola, C.** (2002) Assembling the stratigraphic record: depositional patterns and time-scales in an experimental alluvial basin. *Basin Res.*, **14**, 287–301.
Smith, C. (1998) Modeling high sinuosity meanders in a small flume. *Geomorphology*, **25**, 19–30.
Soulsby, R. (1997) *Dynamics of Marine Sands*. Thomas Telford Publications, London, UK.
Southard, J. (1971) Representation of bed configurations in depth-velocity-size diagrams. *J. Sediment. Petrol.*, **41**, 903–915.
Southard, J.B. and **Boguchwal, A.L.** (1973) Flume experiments on the transition from ripples to lower flat bed with increasing sand size. *J. Sediment. Petrol.*, **43**, 1114–1121.
Southard, J.B. and **Boguchwal, A.L.** (1990) Bed configurations in steady unidirectional water flows. Part 2. Synthesis of flume data. *J. Sediment. Petrol.*, **60**, 658–679.
Southard, J. and **Dingler, J.** (1971) Flume study of ripple propagation behind mounds on flat sand beds. *Sedimentology* **16**, 251–263.
Stefanon, L., **Carniello, L.**, **D'Alpaos, A.** and **Lanzoni, S.** (2010) Experimental analysis of tidal network growth and development. *Cont. Shelf Res.*, **30**, 950–962.
Struiksma, N. and **Klaassen, G.** (1986) Experimental comparison of scaling with sand and bakelite as bed material. IAHR Symposium on Scale effects in modelling sediment transport phenomena, Toronto, ON, Canada.
Swamee, P. and **Ojha, C.** (1991) Drag coefficient and fall velocity of nonspherical particles. *J. Hydraul. Eng.*, **117**, 660–667.
Tal, M. and **Paola, C.** (2010) Effects of vegetation on channel morphodynamics: Results and insights from laboratory experiments. *Earth Surf. Proc. Land.*, **35**, 1014–1028.
Tambroni, N., **Bolla Pittaluga, M.** and **Seminara, G.** (2005) Laboratory observations of the morphodynamic evolution of tidal channels and tidal inlets. *J. Geophys. Res.*, **110**, F04009.
Vendetti, J., **Church, M.** and **Bennett, S.** (2005) On the transition between 2D and 3D dunes. *Sedimentology*, **52**, 1343–1359.
Venditti, J.G., **Church, M.** and **Bennett, S.J.** (2005a) Morphodynamics of small-scale superimposed sand waves over migrating dune bed forms. *Water Resour. Res.* **41**, w10423.
Venditti, J.G., **Church, M.A.** and **Bennett, S.J.** (2005b) Bed form initiation from a flat sand bed. *J. Geophys. Res., series F*, **110**, F01009.
Venditti, J.G., **Church, M.** and **Bennett, S.J.** (2006) On interfacial instability as a cause of transverse subcritical bed forms. *Water Resour. Res.* **42**, w07423.
Vollmer, S. and **Kleinhans, M.G.** (2007) Predicting incipient motion including the effect of turbulent pressure fluctuations in the bed. *Water Resour. Res.*, **43**, W05410.
Wiberg, P. and **Smith, J.** (1987) Calculations of the critical shear stress for motion of uniform and heterogeneous sediments. *Water Resour. Res.*, **23**, 1471–1480.
Yalin, M. (1971) *Theory of Hydraulic Models*. Macmillan, London, UK.
Zanke, U.C.E. (2003) On the influence of turbulence on the initiation of sediment motion. *Int. J. Sediment. Res.*, **18**, 1–15.

Manuscript received 23 May 2016; revision accepted 5 January 2017

APPENDIX

Definition of variables in bedform stability diagrams

Southard & Boguchwal (1990) set up two different diagrams for current bedforms: one based on total bed shear stress and median particle size, and a set of three diagrams based on flow velocity and median particle size for three ranges of flow depth. As is well known, five bed states were distinguished: no movement, ripples, dunes, upper-stage plane bed ('USPB') with sheetflow, and upper-flow regime with plane bed and antidunes. All diagrams were corrected for temperature by adjusting particle size and flow velocity for the temperature-dependent viscosity. However, total bed shear stress includes the form friction caused by the bedforms that the diagram is attempting to predict, which makes this version inconveniently circular. To remove this circularity, van den Berg & van Gelder (1993) employed the bed shear stress partitioning common in sediment transport prediction (here, van Rijn, 1984a).

The Southard & Boguchwal (1990) diagrams plot bed states in Velocity–grain-size space,

© 2017 The Authors. *Sedimentology* published by John Wiley & Sons Ltd on behalf of International Association of Sedimentologists, *Sedimentology*, **64**, 1381–1401

where both variables were corrected for temperature effects on the viscosity of water:

$$u_{t10} = u\left(\frac{\mu}{\rho}\right)^{1/3} \tag{12}$$

where u, flow velocity (m s^{-1}), here for a temperature t = 10°C, where $\mu \approx 4 \times 10^{-5}/(20 + t)$ is the dynamic viscosity (kg sm^{-1}) and ρ = density of water (kg m^{-3}), and:

$$D_{t10} = D_{50}\left(\frac{\mu}{\rho}\right)^{2/3} \tag{13}$$

where D_{50}, median particle size (m). Three versions of the diagram were produced on the basis of data for different ranges of water depth. In an attempt to remove the water depth dependence of the flow velocity diagrams, Southard & Boguchwal (1990) also constructed a diagram based on total bed shear stress versus temperature-corrected particle size:

$$\tau = \rho g h \sin S \tag{14}$$

where g, gravitational acceleration [9·81 m s^{-2}], h, water depth and sin S is the energy gradient. However, the total shear stress is not entirely independent of the bed state that is predicted because it incorporates form-related shear stress.

Van den Berg & van Gelder (1993) removed this element of circularity by using the shear stress related to skin friction only, calculated as:

$$\tau' = \rho g \frac{u^2}{C'^2} \tag{15}$$

where the Chezy coefficient is calculated for the skin friction part only as:

$$C' = 18_{10} \log \frac{12h}{k'_s} \tag{16}$$

where k'_s, Nikuradse roughness length (m) related to the larger particles, where $k'_s = D_{90}$ or $k'_s = 2{\cdot}5D_{50}$ when D_{90} is unknown and henceforth we drop the prime. Note that van den Berg & van Gelder (1993) originally proposed $k_s = 3D_{90}$ but on the basis of Kleinhans & Van Rijn (2002) $k_s = 1D_{90}$ is adopted. Furthermore, van den Berg & van Gelder (1993) made their diagram dimensionless and corrected for temperature effects by using the Bonnefille parameter for particle size on the abscissa:

$$D_* = D_{50}\left(\frac{\rho_s - \rho}{\rho}\frac{g}{\nu^2}\right)^{1/3} \tag{17}$$

where ρ_s, density of sediment (kg m^{-3}) and ν, μ/ρ is the kinematic viscosity (m^2 s^{-1}) depending on temperature (°C). The ordinate has the Shields parameter for bed shear stress related to skin friction:

$$\theta = \frac{\tau'}{(\rho_s - \rho) g D_{50}} \tag{18}$$

van den Berg & Van Gelder (1998) further showed that lines for the transition to critical flow (Froude number ≈ 1) can be plotted at various positions in the diagram depending on the flow depth, where the Froude number is defined as:

$$\mathrm{Fr} = \frac{u}{\sqrt{gh}} \tag{19}$$

As a further frame of reference, a modern empirical version of the Shields curve is plotted to denote the gradual 'threshold' for the beginning of generalized sediment motion (Soulsby, 1997):

$$\theta = \frac{1}{2}\frac{0{\cdot}3}{1 + 1{\cdot}2D_*} + 0{\cdot}055[1 - \exp(-0{\cdot}02D_*)] \tag{20}$$

which plots close to the lowest line below which no sediment motion occurs. Note that the function is here multiplied with 1/2 so that it represents the beginning of motion rather than the beginning of generalized bedload as the original Shields curve does. Based on a description of turbulent flow over grains of natural shapes and earlier work by Wiberg & Smith (1987), Zanke (2003) derived an instructive semi-empirical relation for the beginning of motion that illustrates the importance of near-bed turbulence intensity $u_{\mathrm{rms,b}}$ relative to velocity at the level of particles u_b:

$$\theta_c = \frac{C_0 K \tan(\varphi/1{\cdot}5)}{\left[1 + \frac{1{\cdot}8u_{\mathrm{rms,b}}}{u_b}\right]^2 \left[1 + 0{\cdot}4K\tan(\varphi/1{\cdot}5)\left(\frac{1{\cdot}8u_{\mathrm{rms,b}}}{u_*}\right)\right]} \tag{21}$$

where φ, angle of repose of the sediment. The correction K accounts for cohesion due to the water–grains system (not of added clay) by correcting the angle of repose with the multiplication factor:

© 2017 The Authors. *Sedimentology* published by John Wiley & Sons Ltd on behalf of International Association of Sedimentologists, *Sedimentology*, **64**, 1381–1401

$$K = 1 + \frac{3 \times 10^{-8}}{(\rho_s - \rho)D^2} \quad (22)$$

which only affects grains of $D < 0{\cdot}020$ mm. Based on his formulation for the universal velocity profile in smooth to rough flow, Zanke (2003) derived equations for the ratios of rms near-bed velocities $u_{rms,b}$ (representing turbulence) and the velocity u_b on the protruding part of the grains or the shear velocity; this accounts for the submergence of grains into the laminar sublayer for smaller grains, so that these are more difficult to entrain as is obvious from the falling trend of θ_c with grain size. Finally, Zanke (2003) showed that the Shields curve for coarse sand in flow without turbulence plots an order of magnitude higher than with turbulence, which is the same magnitude as the Shields curve representing finer sands with turbulence damped out by the buffer layer. The transition from smooth to rough bed takes place at the minimum in the Shields curve, which coincides with the ripple–dune transition in the bedform stability diagrams. Vollmer & Kleinhans (2007) extended this work further by including turbulence into the bed and a universal velocity profile with the Van Driest function for the transition from hydraulic smooth to rough conditions.

© 2017 The Authors. *Sedimentology* published by John Wiley & Sons Ltd on behalf of International Association of Sedimentologists, *Sedimentology*, **64**, 1381–1401